ME469 Final Project

Michael Whitmore

June 2021

1 Introduction

In this project a two-dimensional thermal convection loop is simulated in order to assess the nonlinear behavior of the flow. This work follows that of Louisos et al. [2] to study the behavior of the system in three Rayleigh-number regimes, including stable convection, chaotic convection with reversals, and aperiodic stable convection. The flow geometry is modeled as a 2D annulus that is heated by constant heat fluxes into and out of the system on the bottom and top half respectively.

The basic mechanism driving this flow is simple. The heat flux in the bottom half of the loop causes the fluid to get hotter. As the fluid in the bottom half of the loop gets hotter, a buoyant force is generated that accelerates the fluid along the azimuthal direction. Depending on the Rayleigh number, this thermally-induced convection can generate a range of different flow behaviors.

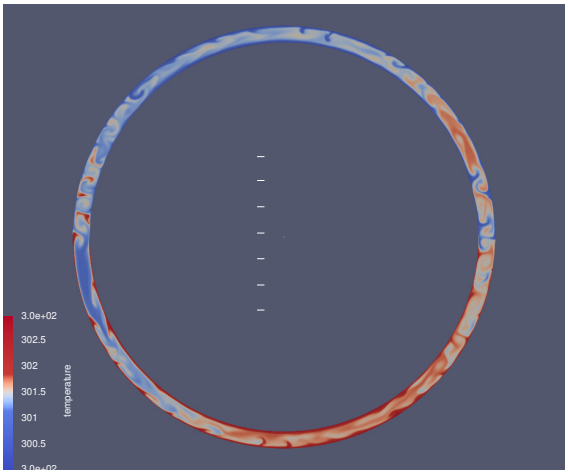

Figure 1: Instantaneous temperature field of the flow with $q'' = 200$ W/m^2 at the time of flow reversal.

The domain has an inner diameter of 69 cm and an outer diameter of 75 cm. The system is modeled using the low-Mach limit of the compressible flow equations along with an enthalpy transport equation. The buoyancy force is modeled in the momentum equation using the Boussinesq approximation. The enthalpy equation is closed using a turbulent Prandtl number to find the thermal diffusivity. The equation set used here assumes constant density and flow properties. These properties are set to the values for liquid water at a 300 K reference temperature.

2 Methodology

The flow is simulated using the NaluCFD [1] solver with a control volume finite element method (CVFEM). The baseline computational grid has approximately 30,000 elements. Time integration is handled by a second order backward difference scheme. The enthalpy transport uses a flux limiter to prevent the local temperature from spuriously dropping below the reference temperature. A no slip boundary condition is

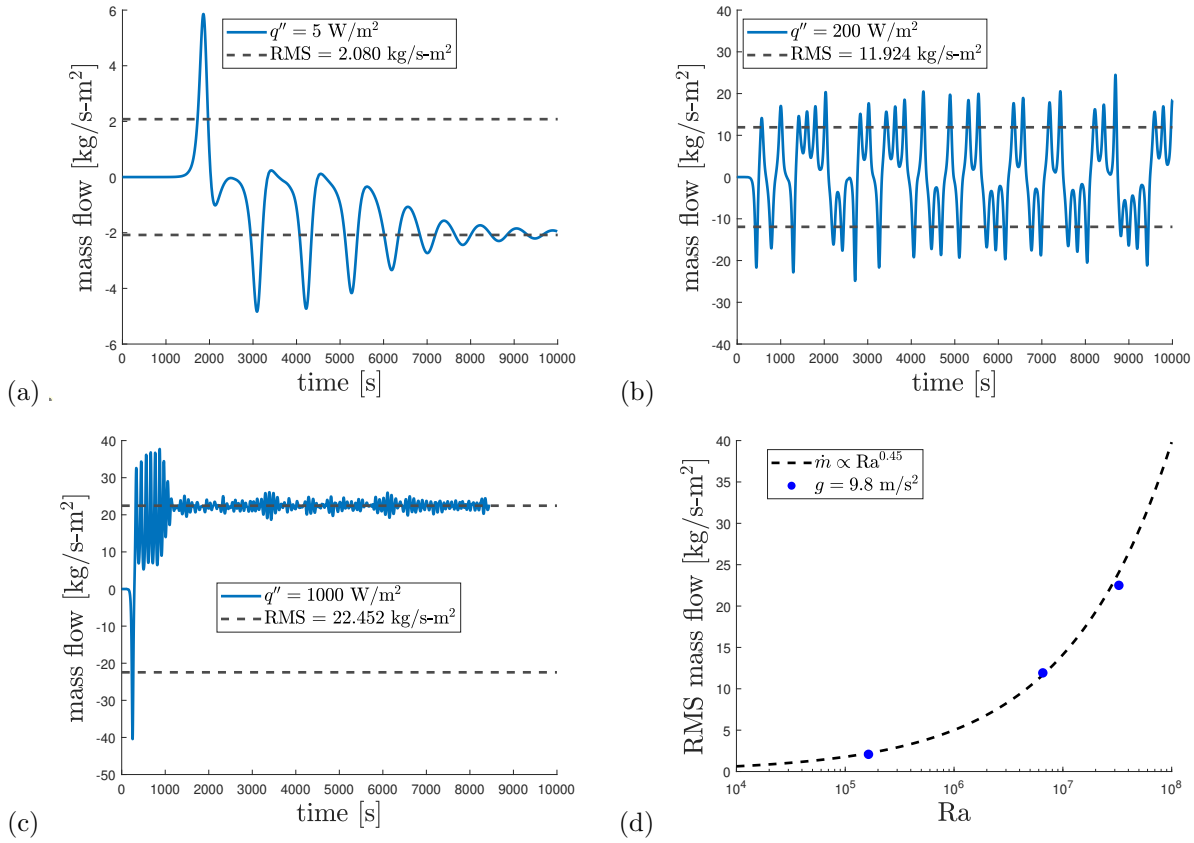

Figure 2: Mass flow rates in time for (a) $q'' = 5$ W/m^2, (b) $q'' = 200$ W/m^2, and (c) $q'' = 1000$ W/m^2. (d) RMS mass flow rate against Rayleigh number is compared with the scaling observed by Louisos et al.

used for the velocities and a constant heat flux boundary condition is used for enthalpy. The specified heat flux is positive, into the system, on both walls in the bottom half of the domain and negative, out of the system, on both walls in the top half of the domain.

The Rayleigh number quantifies the ratio of buoyancy forces to viscous forces. For a constant heat flux with the Boussinesq approximation, it can be written as

$$\mathrm{Ra} = \frac{\rho g \beta L^4}{\mu \alpha k} q'', \tag{1}$$

where ρ is the fluid density, g is the gravitational acceleration, β is the thermal expansion coefficient, L is the characteristic length scale, μ is the dynamic viscosity, α is the thermal diffusivity, k is the thermal conductivity, and q'' is the heat flux per unit area. The length scale L for this case is chosen as the annulus thickness, 3 cm, since this is the scale of the temperature gradients.

Louisos et al. observed that for different Rayleigh number regimes, the flow dynamics changed significantly. For the range of $10^3 < \mathrm{Ra} < 5.8 \times 10^5$ stable convection was observed, where the oscillations in mass flow rate are damped. The range of $5.8 \times 10^5 < \mathrm{Ra} < 1.4 \times 10^7$ showed a chaotic convection behavior with flow reversals. Above $\mathrm{Ra} > 1.4 \times 10^7$ stable aperiodic convection was observed. For the present cases, using $g = 9.81$ m/s^2, three heat fluxes are chosen: 5 W/m^2, 200 W/m^2, and 1000 W/m^2. These heat fluxes correspond to Rayleigh numbers 1.6×10^5, 6.5×10^6, and 3.3×10^7 respectively. These heat fluxes were chosen in order to assess the flow behavior in the stable convection, chaotic convection, and high Rayleigh regimes.

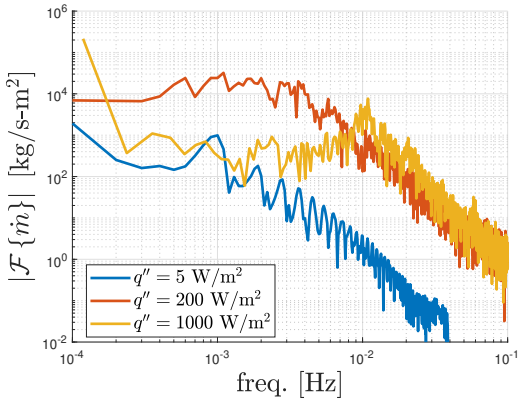

Figure 3: Mass flow rate spectrum for three cases.

3 Results

3.1 Quantities of interest

The average azimuthal mass flow rate is computed from simulation data as a function of time. The results are shown in Figure 2(a-c). Looking at the time resolved behavior of the mean flow, it is seen that the lowest Rayleigh number case has a stable oscillatory behavior that is converging to a mass flow rate of 2.1 kg/s-m^2. In contrast the intermediate Rayleigh number case is showing an oscillatory behavior that is undamped and chaotically reversing direction. This case is converging to a root mean square mass flow rate of 11.9 kg/s-m^2. The high Rayleigh number case has fast, small scale oscillations that are not entirely damped but the overall flow is converging to a statistically stationary mass flow rate of 22.5 kg/s-m^2. Figure 2(d) compares the RMS mass flow rates to the Rayleigh number scaling quoted by Louisos et al. Reasonable agreement is seen for the scaling of Ra$^{0.45}$.

The mass flow rate spectra are shown in Figure 3. It is seen that the low Rayleigh number case has a peak around 10^{-3} Hz, corresponding to it's dominant oscillatory mode. The high Rayleigh number case has a peak around 10^{-2} Hz corresponding to the dominant oscillatory mode. This agrees with the qualitative behavior seen that the high Rayleigh number case has more small, fast scale oscillations. The intermediate Rayleigh number case has a poorly defined peak around 4×10^{-3} Hz which corresponds to its oscillation that repeats about 4 times every 1000 seconds. It also has peaks at lower frequencies which correspond to the flow reversal behavior, which happens chaotically, but on a slower time scale, only about 1-2 times every 1000 seconds. These spectral results show a qualitative agreement with the results of Louisos et al. to quantify the dominant oscillatory mode in the mass flow rate, however for the present intermediate Rayleigh number result, the corresponding mode is not strongly dominant in the spectrum. This, however could just be an artifact of spectral resolution since the dominant peaks shown for chaotic convection in Louisos et al. are very narrow and the low frequency part of the spectrum is also relatively flat.

It is important to note that, when comparing to the results of Louisos et al., the results are not non-dimensionalized. Because of this, even though the parameters are nominally chosen for water at 300 K, there is some uncertainty in the exact values of the parameters used. This ambiguity of the flow parameters results in about 5-10% relative difference in the mass flow rates since the matching heat fluxes may give slightly different Rayleigh numbers. As a result, direct quantitative comparison is not made against the Louisos et al. mass flow rates.

3.2 Sensitivity to mesh resolution

The $q'' = 5$ W/m^2 case is simulated on a refined grid to assess the sensitivity to mesh resolution. This case is chosen to assess mesh refinement due to its lower computational cost. The finer mesh has approximately 120,000 elements, which constitutes a roughly 2× isotropic refinement from the baseline grid. The mass flow rate in time for the refined flow case is shown in Figure 4(a). The difference in RMS mass flow is

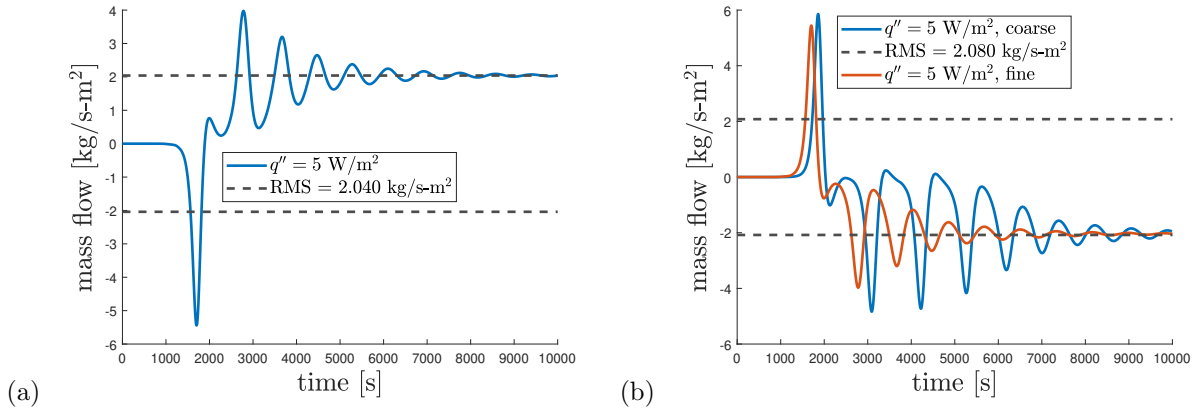

Figure 4: Mass flow rates of the $q'' = 5$ W/m^2 case for the (a) refined mesh and the (b) comparison at coarse and fine meshes. The refined mesh is flipped in (b) for comparison with the coarse case.

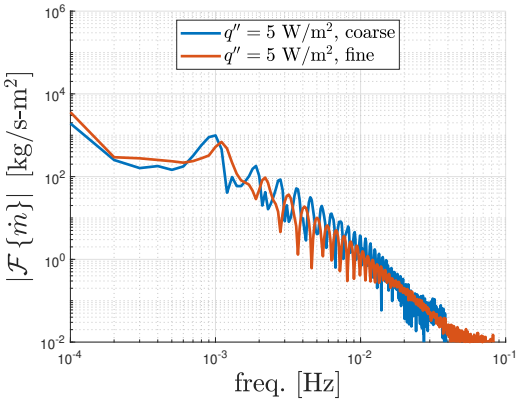

Figure 5: Mass flow rate spectrum of the $q'' = 5$ W/m^2 case for two different mesh resolutions.

approximately 1% suggesting that RMS mass flow is reasonably grid converged for this case. The spectral peak around frequency 10^{-3} Hz has a larger relative difference of $\sim 10\%$. This suggests the frequency of oscillation is more difficult to converge.

Looking at the time history of the mass flow rates, it is seen that the refined case diverges from the coarse case at early time and converges to convection in the opposite direction. This suggests the initial numerical perturbation is different enough to push the flow in the opposite direction. Additionally, the initial flow transients appear to damp much more quickly at the finer mesh resolution.

The mesh sensitivities of the higher Rayleigh number cases are omitted due to the larger computational expense. These cases reach higher local Reynolds numbers and require much smaller time steps to resolve the dynamics. It is not expected, however, that these results would be sensitive to mesh resolution. This is assumed based on their mass flow spectra which show that the spectral content decays significantly before reaching the smallest resolved frequencies. This suggests that the scales smaller than the grid scales are not important to capture the quantities of interest.

3.3 Computational cost

For the low Rayleigh number case, it was observed that the computation took about 4.0 seconds per time step per million elements. For the higher Rayleigh numbers, this increased to about 4.7 seconds per time step per million elements. This increase in computation time was due to the momentum and enthalpy systems being harder to solve, requiring more linear iterations per time step. In general, it was observed that the

code spent most of the time setting up preconditioners for the continuity equation. This accounted for 47-57% of the computation time overall. The next closest computational expenses were the solution steps for continuity, momentum, and enthalpy equation systems, each accounting for roughly 10% of the computation time overall.

4 Conclusions

A two-dimensional thermal convection loop is simulated for three Rayleigh numbers. The three Rayleigh numbers are chosen to in order to assess the flow behavior in the stable convection regime, the chaotic convection regime, and the stable, aperiodic, high Rayleigh number regime. The results of the simulations show qualitative agreement with the work of Louisos et al. for the prediction of the time resolved mass flow rate, root mean square mass flow rate, and dominant modes of the mass flow rate spectrum. The root mean square mass flow rates are in agreement with the Rayleigh number scaling quoted by Louisos et al. The quantities of interest do not show a strong sensitivity to mesh refinement for the lowest Rayleigh number case. The mesh refinement studies for the higher Rayleigh number cases are omitted due to computational expense, however it is assumed that the quantities of interest for these cases would also be weakly sensitive to the mesh resolution due to the decay of their mass flow rate spectra at high frequencies.

References

[1] Domino, S."Sierra Low Mach Module: Nalu Theory Manual 1.0", SAND2015-3107W, Sandia National Laboratories Unclassified Unlimited Release (UUR), 2015. https://github.com/NaluCFD/NaluDoc

[2] Louisos, W. F., Hitt, D. L., Danforth, C. M., "Chaotic flow in a 2D natural convection loop with heat flux boundaries", International Journal of Heat and Mass Transfer, 61, pp. 565-576, 2013.